Thermoelectric properties of $(Bi_{0.25}Sb_{0.75})_2Te_3$ alloys fabricated by hot-pressing method

DOW-BIN HYUN, JONG-SEUNG HWANG, JAE-DONG SHIM
Metal Processing Research Center, Korea Institute of Science and Technology, Seoul 136-791, South Korea
E-mail: dbhyun@kist.re.kr

TAE SUNG OH
Dept. of Metallurgical Engineering and Materials Science, Hong Ik University, Seoul 121-791, South Korea

Thermoelectric properties of the hot-pressed p-type $(Bi_{0.25}Sb_{0.75})_2Te_3$ alloy were characterized with variation of the hot-pressing temperature and the starting powder size. The roles of the factors which affect the Seebeck coefficient of the hot-pressed $(Bi_{0.25}Sb_{0.75})_2Te_3$ alloy has been elucidated in this study. The donor-like behavior of oxygen could be one of the possible explanations for the higher Seebeck coefficient of the hot-pressed $(Bi_{0.25}Sb_{0.75})_2Te_3$ alloy. Te vacancies formed by mechanical deformation during the powdering process significantly promote the diffusion of second phase Te atoms into their lattice sites so that the matrix Te solubility approaches its equilibrium value at a given temperature in a relatively short length of time. Using the Seebeck coefficient at various hot-pressing temperatures, the micro-phase diagram near the stoichiometric composition of $(Bi_{0.25}Sb_{0.75})_2Te_3$ was evaluated.

1. Introduction

Thermoelectric cooling modules have been widely applied to cool electronic devices, such as integrated circuit packages, high-power laser diodes, and IR detectors, because quick and precise control of temperature is possible with almost no noise during operation [1, 2]. As p-type materials for thermoelectric cooling modules, Bi_2Te_3–Sb_2Te_3 single crystals have been extensively investigated, and the thermoelectric figure-of-merit of Bi_2Te_3–Sb_2Te_3 was optimized with the composition of $(Bi_{0.25}Sb_{0.75})_2Te_3$ [1–4]. However, Bi_2Te_3–Sb_2Te_3 single crystals have very poor mechanical properties due to the cleavage fracture along the basal plane of the rhombohedral structure. As a new processing technique, thus, hot-pressing method has been applied to prepare p-type Bi_2Te_3–Sb_2Te_3 sintered materials in recent years [4–9].

In this study, p-type $(Bi_{0.25}Sb_{0.75})_2Te_3$ alloy powders were hot-pressed at temperatures ranging from 300°C to 550°C, and the thermoelectric properties were characterized with variation of the hot-pressing temperature and the powder size. Effects of several factors, such as Te evaporation, oxidation and mechanical deformation during the powdering process, and Te solubility, on the Seebeck coefficient of the hot-pressed $(Bi_{0.25}Sb_{0.75})_2Te_3$ alloy were also investigated.

2. Experimental

To prepare the $(Bi_{0.25}Sb_{0.75})_2Te_3$ powders using melting/grinding method, high purity (>99.99%) Bi, Sb and Te granules were weighted to make an ingot of 40 g and charged into a carbon-coated quartz tube. The quartz tube was vacuum-sealed at 10^{-5} torr. Bi, Sb and Te in the quartz tube were melted and homogeneously mixed at 800°C for 5 hours using a rocking furnace, and then quenched to room temperature. The $(Bi_{0.25}Sb_{0.75})_2Te_3$ ingots were crushed in an alumina mortar and sieved to obtain the powders of under 38 μm, 38–90 μm and 90–250 μm.

To prepare the $(Bi_{0.25}Sb_{0.75})_2Te_3$ powders using mechanical alloying, appropriate amounts of Bi, Sb and Te were weighed and charged with 0.3 wt % excess Te into an attrition mill under Ar atmosphere. Zirconia balls were used as a milling media and ball-to-powder ratio was held at 50 : 1. Mechanical alloying was performed by rotating the alumina container at about 300 rpm for 20 hours. After the attrition milling process, X-ray diffraction (XRD) analysis was performed to complete formation of the alloy powders. Differential Thermal Analysis (DTA) was performed in Ar atmosphere at a scan rate of 5°C/min for the as-mixed and mechanically alloyed powders.

The powders fabricated by the melting/grinding and mechanical alloying processes were cold-pressed at 425 MPa to form $5 \times 5 \times 12$ mm^3 compacts, and hot-pressed in a vacuum for 30 minutes at temperatures ranging from 300°C to 550°C. The Seebeck coefficient (α) was measured by applying a temperature difference of 10°C at both ends of the specimen. The electrical resistivity (ρ) and the figure-of-merit (Z) were measured using the Harman method [10] at 10^{-5} torr to minimize the

0022–2461

thermal conduction through convection. The thermal conductivity (κ) was determined using the relationship of $\kappa = \alpha^2/(Z \cdot \rho)$. The error range of the measurement values was within 5%.

3. Results

XRD patterns of the as-mixed and mechanically alloyed powders, shown in Fig. 1, clearly illustrated the formation of $(Bi_{0.25}Sb_{0.75})_2Te_3$ alloy from elemental Bi, Sb and Te powders by mechanical alloying at room temperature. DTA curves of the as-mixed and mechanically alloyed $(Bi_{0.25}Sb_{0.75})_2Te_3$ powders are shown in Fig. 2a and b. For the as-mixed powder, endothermic peaks were observed at 272°C, 423°C and 617°C due to the melting of Bi, Te-rich (Bi,Sb)-Te eutectic and $(Bi_{0.25}Sb_{0.75})_2Te_3$. Exothermic peak at 531°C was due to the formation of $(Bi_{0.25}Sb_{0.75})_2Te_3$. Such peaks except one at 617°C disappeared in DTA for mechanically alloyed powder, which indicated the formation of $(Bi_{0.25}Sb_{0.75})_2Te_3$ solid solution by mechanical alloying at room temperature. Endothermic peak at 417°C was due to the formation of Te-rich (Bi,Sb)-Te eutectic liquid phase [11]. Particle size distribution of the mechanically alloyed $(Bi_{0.25}Sb_{0.75})_2Te_3$ powders, shown in Fig. 3, revealed a bimodal distribution consisted of the powders smaller than 0.1 μm and the powders larger than 1 μm. As mechanical alloying occurs by repeated fracture and cold-welding of the powders during high energy milling process, it produces fine-grained powders [12–14]. The powders with the size larger than 1 μm are thought to be the agglomerates of the powders. Thus, the $(Bi_{0.25}Sb_{0.75})_2Te_3$ powders prepared for hot- pressing in this study could be classified as four different sizes of <1 μm, <38 μm, 38–90 μm, and 90–250 μm.

The Seebeck coefficient of the hot-pressed $(Bi_{0.25}Sb_{0.75})_2Te_3$ alloys, measured at room temperature, is shown in Fig. 4. The Seebeck coefficient of the

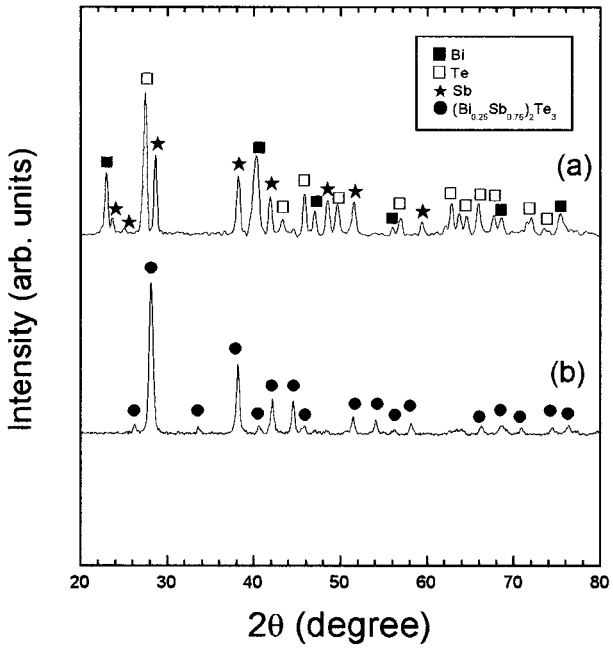

Figure 1 X-ray diffraction patterns of (a) as-mixed and (b) mechanically alloyed $(Bi_{0.25}Sb_{0.75})_2Te_3$ powders.

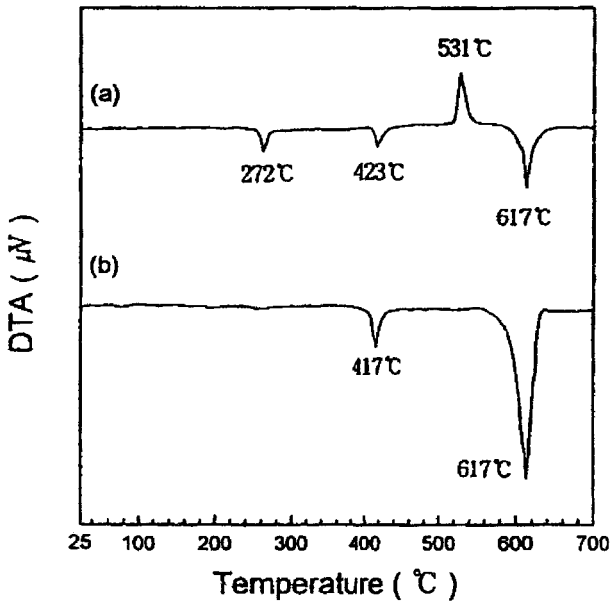

Figure 2 DTA curves of (a) as-mixed and (b) mechanically alloyed $(Bi_{0.25}Sb_{0.75})_2Te_3$ powders.

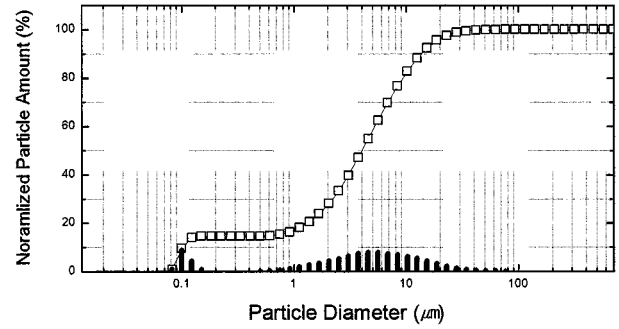

Figure 3 Particle size distribution of $(Bi_{0.25}Sb_{0.75})_2Te_3$ powders fabricated by mechanical alloying.

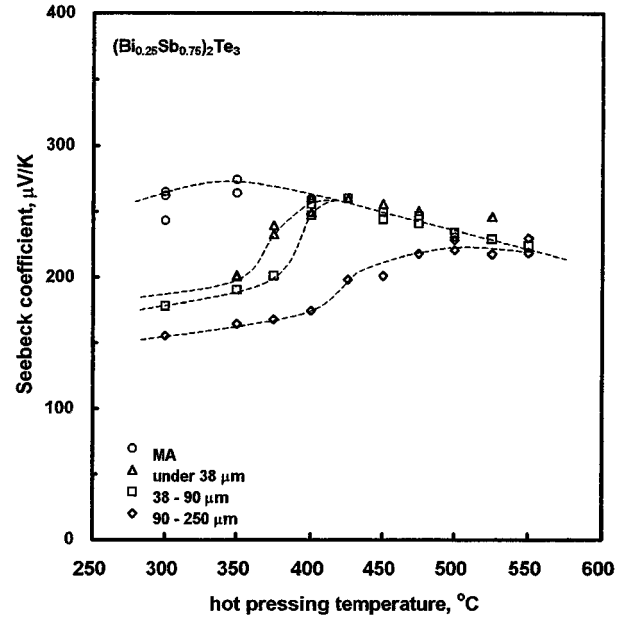

Figure 4 Seebeck coefficient of $(Bi_{0.25}Sb_{0.75})_2Te_3$ as a function of hot-pressing temperature.

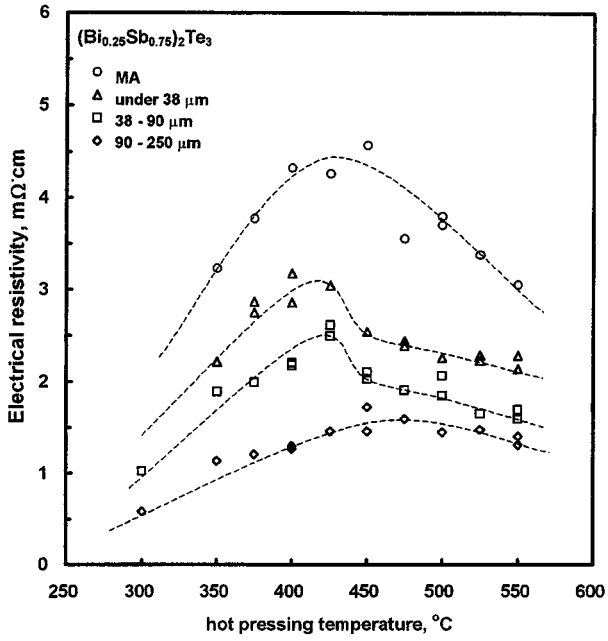

Figure 5 Electrical resistivity of $(Bi_{0.25}Sb_{0.75})_2Te_3$ as a function of hot-pressing temperature.

hot-pressed specimens increased with increasing the hot-pressing temperature, reaching maximum, and then decreased with further increase of the hot-pressing temperature. With increasing the powder size, the Seebeck coefficient before reaching its maximum was lower and the hot-pressing temperature for the maximum Seebeck coefficient shifted to higher temperature. After reaching the maximum Seebeck coefficient, however, the degree of the Seebeck coefficient decrement with increasing the hot-pressing temperature was identical without depending on the powder size.

The electrical resistivity of $(Bi_{0.25}Sb_{0.75})_2Te_3$ with hot-pressing temperature is shown in Fig. 5. The electrical resistivity of the hot-pressed $(Bi_{0.25}Sb_{0.75})_2Te_3$ increased with increasing hot-pressing temperature, reached a maximum value, and then decreased with further increase of the hot-pressing temperature. However, the electrical resistivity of the specimens hot-pressed with the powder of $<38\ \mu$m and 38–90 μm size showed abrupt decrease between 425°C and 450°C. Assuming the Boltzmann distribution, the relationship between the Seebeck coefficient and the electrical resistivity at room temperature can be expressed by Equation 1 [15].

$$\alpha = \pm\frac{k_B}{e}\left[s + \frac{5}{2} + \ln\frac{2\left(2\pi m^* k_B T\right)^{3/2}}{ph^3}\right] = \pm\frac{k_B}{e}[s + \ln\rho] + C \quad (1)$$

In Equation 1, k_B is Boltzmann's constant, e the electronic charge, s the scattering parameter, m^* the effective mass, p the hole concentration, h the Planck's constant and C a constant. Equation 1 shows that the Seebeck coefficient is directly related to the electrical resistivity when the scattering parameter is the same. As shown in Fig. 5, the electrical resistivity was lowered with increasing the powder size. The Seebeck coefficient of the specimens hot-pressed at temperatures higher than 425°C with the powders of $<1\ \mu$m, $<38\ \mu$m, and 38–90 μm size, however, was not affected by the powder size as shown in Fig. 4. The relative densities of $(Bi_{0.25}Sb_{0.75})_2Te_3$ hot-pressed with the powders of $<1\ \mu$m, $<38\ \mu$m, and 38–90 μm size were 89.3%, 92.0% and 94.1%, respectively, i.e. the porosity of the hot-pressed specimens increased with decreasing powder size. For the materials with void ratio of υ_d, the electrical resistivity can be expressed as Equation 2, while the Seebeck coefficient is not affected by the void ratio [16].

$$\rho = \rho_o[(1 + \upsilon_d)/(1 - \upsilon_d)] \quad (2)$$

In Equation 2, ρ_o is the electrical resistivity of the void-free materials. The Seebeck coefficient of p-type thermoelectric materials is related to the hole concentration as Equation 1. Thus, identical Seebeck coefficient implied the same hole concentrations for the specimens hot-pressed at temperatures higher than 425°C with the powders of $<1\ \mu$m, $<38\ \mu$m, and 38–90 μm size. Then, the increase of the electrical resistivity with decreasing the powder size is probably due to the reduction of the mobility by carrier scattering at voids.

The thermal conductivity of $(Bi_{0.25}Sb_{0.75})_2Te_3$ with hot-pressing temperature is shown in Fig. 6. The thermal conductivity decreased with increasing the hot-pressing temperature up to about 500°C, and then increased with further increase of the hot-pressing temperature. According to the Fermi-Dirac distribution, the Seebeck coefficient and electronic thermal conductivity (κ_{el}) can be expressed as Equations 3 and 4, respectively [15].

$$\alpha = \pm\left(\frac{k_B}{e}\right)\left[\frac{(s + 5/2)F_{s+3/2}(\xi)}{(s + 3/2)F_{s+1/2}(\xi)} - \xi\right] \quad (3)$$

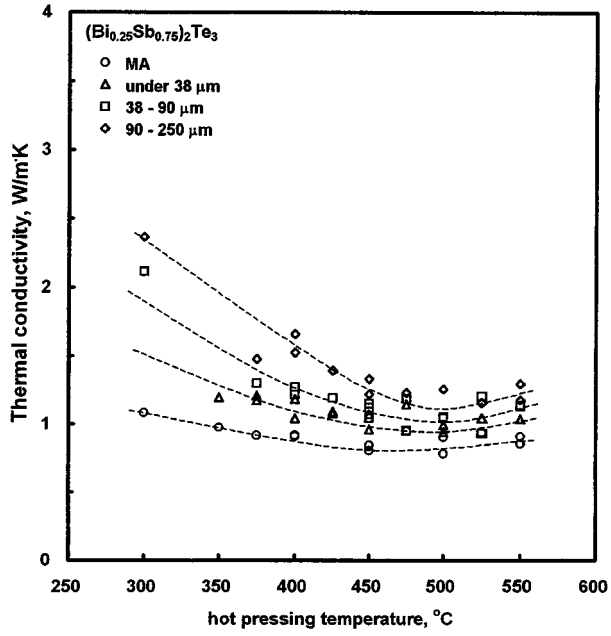

Figure 6 Thermal conductivity of $(Bi_{0.25}Sb_{0.75})_2Te_3$ as a function of hot-pressing temperature.

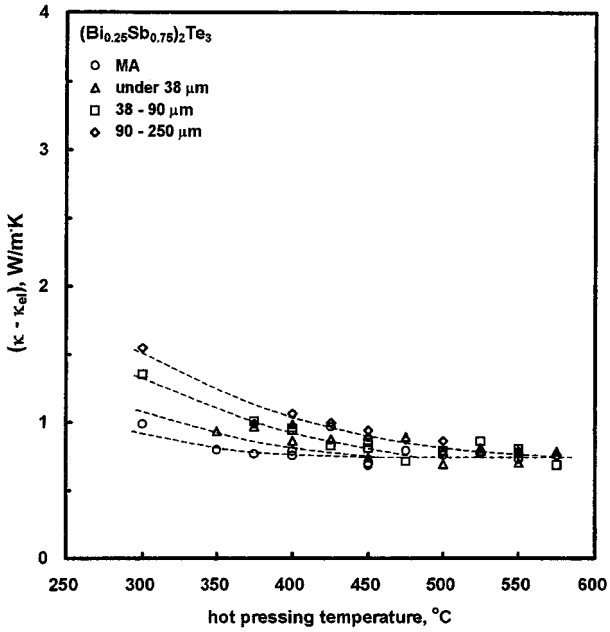

Figure 7 $(\kappa - \kappa_{el})$ of $(Bi_{0.25}Sb_{0.75})_2Te_3$ as a function of hot-pressing temperature.

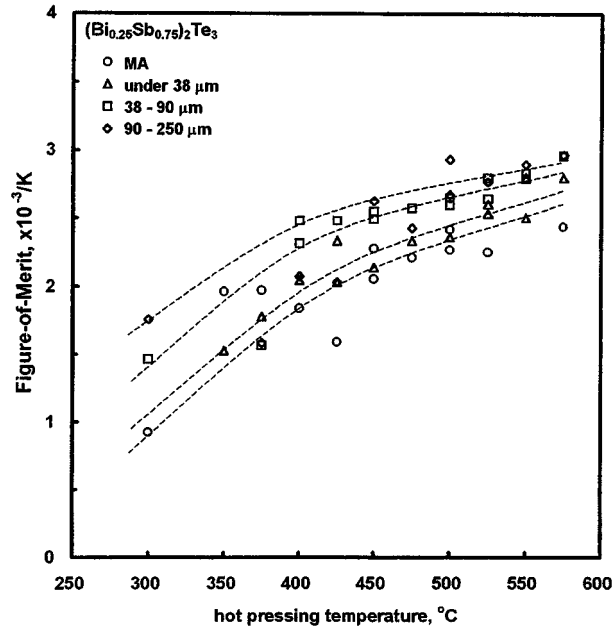

Figure 8 Figure-of-merit of $(Bi_{0.25}Sb_{0.75})_2Te_3$ as a function of hot-pressing temperature.

$$\kappa_{el} = L\sigma T = \left\{ \frac{(s+7/2)F_{s+5/2}(\xi)}{(s+3/2)F_{s+1/2}(\xi)} - \left[\frac{(s+5/2)F_{s+3/2}(\xi)}{(s+3/2)F_{s+1/2}(\xi)} \right]^2 \right\} \left(\frac{k_B}{e} \right)^2 \sigma T \quad (4)$$

In Equations 3 and 4, ξ is the reduced Fermi energy and $F_t(\xi)$ is the Fermi integral defined as Equation 5.

$$F_t(\xi) = \int_0^\infty \frac{x^t\, dx}{1 + \exp(x - \xi)} \quad (5)$$

Assuming scattering parameter $s = 0$, the reduced Fermi energy was calculated from the Seebeck coefficient shown in Fig. 4, and then electronic thermal conductivity was calculated using the reduced Fermi energy and the electrical resistivity shown in Fig. 5. $(\kappa - \kappa_{el})$ of the $(Bi_{0.25}Sb_{0.75})_2Te_3$ alloy with hot-pressing temperature is shown in Fig. 7. For the specimens hot- pressed at temperatures above 375°C with the powders of <1 μm size, $(\kappa - \kappa_{el})$ showed constant value of 0.78 watt/m·K. Although the specimens hot-pressed with coarser powders showed higher $(\kappa - \kappa_{el})$ values at lower temperature range, $(\kappa - \kappa_{el})$ of all specimens approached the same value with increasing the hot-pressing temperature. For the materials with void ratio of υ_d, the thermal conductivity can be expressed as Equation 6 [16].

$$\kappa = \kappa_o[(1 - \upsilon_d)/(1 + \upsilon_d)] \quad (6)$$

In Equation 6, κ_o is the thermal conductivity for the void-free materials. Thus, the decrease of $(\kappa - \kappa_{el})$ with decreasing powder size would be due to the larger void ratio of the specimens hot-pressed with finer powders.

As shown in Fig. 8, the figure-of-merit $(Z = \alpha^2/\rho \cdot \kappa)$ of the hot-pressed $(Bi_{0.25}Sb_{0.75})_2Te_3$ increased with increasing the hot-pressing temperature, and a maximum value of 2.9×10^{-3}/K was obtained by hot-pressing the powders of 90–250 μm size at 550°C. Regardless of the powder size, the Seebeck coefficient and $(\kappa - \kappa_{el})$ showed almost same values at higher hot-pressing temperatures. Thus, the increase of the figure-of-merit with increasing the powder size was attributed to the lower electrical resistivity with higher density of the hot-pressed sinters.

4. Discussion

The Seebeck coefficient of an as-solidified $(Bi_{0.25}Sb_{0.75})_2Te_3$ ingot was 132 μV/K and that of the cold-pressed compacts were 145–163 μV/K as summarized in Table I. After hot-pressing, however, the Seebeck coefficient increased up to about 250 μV/K as shown in Fig. 4. In this work, we have discussed the role of several factors which affect the Seebeck coefficient of the hot-pressed $(Bi_{0.25}Sb_{0.75})_2Te_3$ alloy.

4.1. Evaporation of tellurium

For Bi_2Te_3–Sb_2Te_3 pseudo-binary alloy, the excess bismuth and antimony occupy tellurium sites and act as

TABLE I Seebeck coefficient of the as-solidified ingot and the cold-pressed compacts

	powder processing	powder size	Seebeck coefficient
as-solidified ingot	-	-	132 μV/K
cold-pressed compact	mechanical alloying	<1 μm	165 μV/K
	pulverizing of ingot	<38 μm	155 μV/K
		38–90 μm	151 μV/K
		90–250 μm	145 μV/K

an acceptor [17]. If evaporation of Te occurs significant during the hot-pressing process, the degree of antistructure defects would increase and hence the Seebeck coefficient would decrease due to the increased hole concentration. Contrary to this, the Seebeck coefficient increased up to 250 μV/K with hot-pressing from 145–163 μV/K of the cold-pressed compact. With this result, it could be thought that evaporation of Te would not be significant to affect the carrier concentration during hot-pressing at temperatures lower than 550°C.

4.2. Effect of oxygen

During the powdering process such as pulverizing of the ingot or mechanical alloying, the powders are heavily deformed and oxygen can be absorbed on the activated surface even in an atmosphere of low oxygen pressure. This absorbed oxygen can easily diffuse into the matrix due to the increased vacancy concentration and dislocation density of the heavily deformed powders. The solubility of oxygen in Bi_2Te_3 is known to be about 0.01 at % [18]. Schultz *et al.* [19] reported that the oxygen dissolved in the $(Bi,Sb)_2Te_3$ lattice have an effect to add donor levels.

To examine the effects of oxygen on the thermoelectric properties, mechanically alloyed $(Bi_{0.25}Sb_{0.75})_2Te_3$ powders were reduced in (50% H_2 + 50% Ar) atmosphere at 400°C for 24 hours and then hot-pressed at 550°C for 30 minutes in vacuum. The hole concentration of the hot-pressed $(Bi_{0.25}Sb_{0.75})_2Te_3$ increased from $1.23 \times 10^{19}/cm^3$ to $1.44 \times 10^{19}/cm^3$ after hydrogen reduction, while that of single crystal was $5.63 \times 10^{19}/cm^3$. The Seebeck coefficient and the electrical resistivity were also changed after hydrogen reduction of the powders as summarized in Table II. The donor-like behavior of oxygen could be one of the possible explanations for higher Seebeck coefficient of the hot-pressed $(Bi_{0.25}Sb_{0.75})_2Te_3$. However, the effect of dissolved oxygen could not explain the variation of the Seebeck coefficient with the hot-pressing temperature as shown in Fig. 4.

4.3. Effect of mechanical deformation

To examine the effects of the mechanical deformation on the thermoelectric properties, six specimens of $5 \times 5 \times 10$ mm^3 size were cut from an as-solidified $(Bi_{0.25}Sb_{0.75})_2Te_3$ ingot and deformed by cold-pressing at 700 MPa, as illustrated in Fig. 9. To maximize the mechanical deformation, the specimen was then rotated 90° and cold-pressed again. Such cold-pressing process was conducted for 1–11 times to change the amount of mechanical deformation, and then the cold-pressed specimens were hot-pressed at 500°C for 30 minutes. The Seebeck coefficient before and after hot-pressing are shown in Fig. 10. The Seebeck coefficient of the cold-pressed specimen increased slightly up to about 150 μV/K with increasing the number of cold-pressing process, i.e. the amount of mechanical

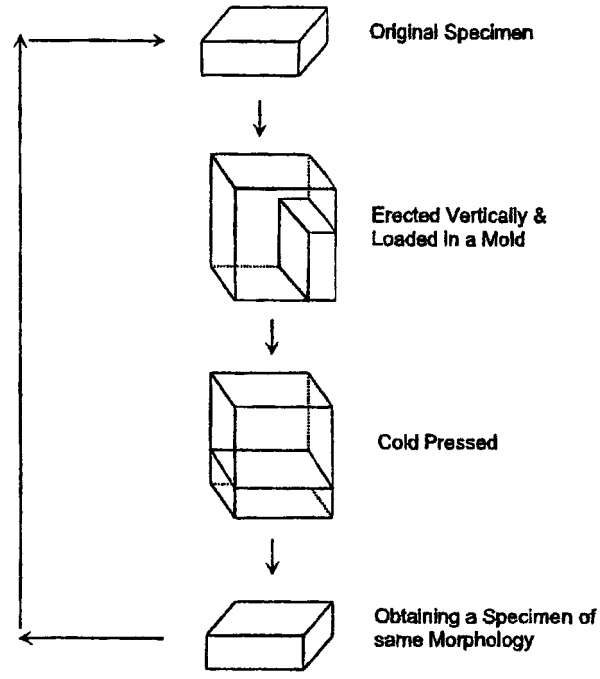

Figure 9 Procedure of cold-pressing.

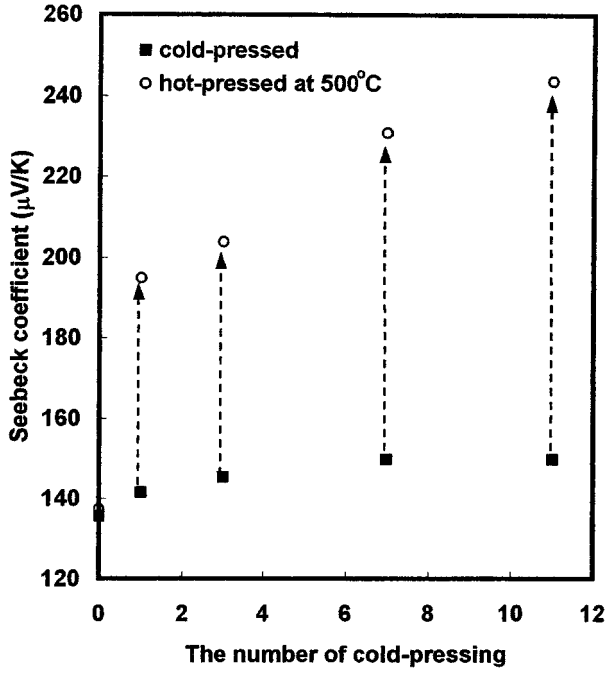

Figure 10 Effect of mechanical deformation on the Seebeck coefficient of $(Bi_{0.25}Sb_{0.75})_2Te_3$.

TABLE II Effect of hydrogen reduction of the powder on the thermoelectric properties of $(Bi_{0.25}Sb_{0.75})_2Te_3$

	carrier concentration [$\times 10^{19}/cm^3$]	Seebeck coefficient [μV/K]	electrical resistivity [m$\Omega \cdot$ cm]	thermal conductivity [W/m $\cdot$ K]	figure-of-merit [$\times 10^{-3}$/K]
mechanically alloyed	1.23	239.0	2.273	0.9146	2.76
reduction treated	1.44	227.2	1.671	1.1533	2.80

deformation. Schultz *et al*. [19] reported that the conduction mechanism of the heavily deformed Bi_2Te_3 single crystal was changed from p-type to n-type due to the generation of Te vacancies (V_{Te}) which act as donors. Thus, the increase in the Seebeck coefficient of the cold-pressed specimens was attributed to the reduction of the hole concentration by compensation with electrons generated by Te vacancies.

In Fig. 10, it should be noted that the effect of mechanical deformation was revealed more significantly after hot-pressing. For the as-solidified specimen without cold-pressing process, the Seebeck coefficient was little changed after hot-pressing. However, the Seebeck coefficient of the mechanically deformed specimens increased remarkably after hot-pressing, and the increment of the Seebeck coefficient with hot-pressing was enlarged for the heavily deformed specimens. The possibility of the Seebeck coefficient change due to the donor-like behavior of Te vacancies could be excluded as they would be annealed out during hot-pressing at 500°C. Thus, it can be concluded that the dislocations and Te vacancies, produced by the mechanical deformation, would promote the diffusion of second phase Te atoms into their own lattice sites during hot-pressing, and result in the increase of the Seebeck coefficient with inhibition of the formation of acceptor-like antistructure defects.

4.4. Effect of tellurium solubility

Four specimens were cut from the as-solidified $(Bi_{0.25}Sb_{0.75})_2Te_3$ ingot and plastically deformed by cold-pressing as illustrated in Fig. 9. The as-solidified and cold-pressed specimens were then annealed at 350°C. Fig. 11 illustrates the Seebeck coefficients of the as-solidified and mechanically deformed specimens with annealing time. The Seebeck coefficient of the as-solidified specimen was not changed even after annealing for 48 hours. However, the Seebeck coefficient of the mechanically deformed specimens increased with increasing the annealing time, and reached to a constant value of about 260 μV/K which is identical to the value obtained for the mechanically alloyed powders as shown in Fig. 4. The only difference between these two specimens is whether they are made of bulk or powders. Therefore, this result also indicates that the stored energy, induced by the mechanical deformation, enhances free Te diffusion into the matrix and promotes the matrix to reach its equilibrium solubility.

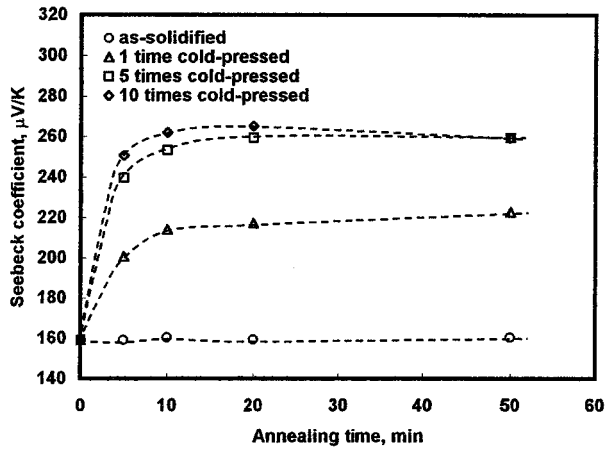

Figure 11 Effect of annealing time on the Seebeck coefficient of mechanically deformed $(Bi_{0.25}Sb_{0.75})_2Te_3$.

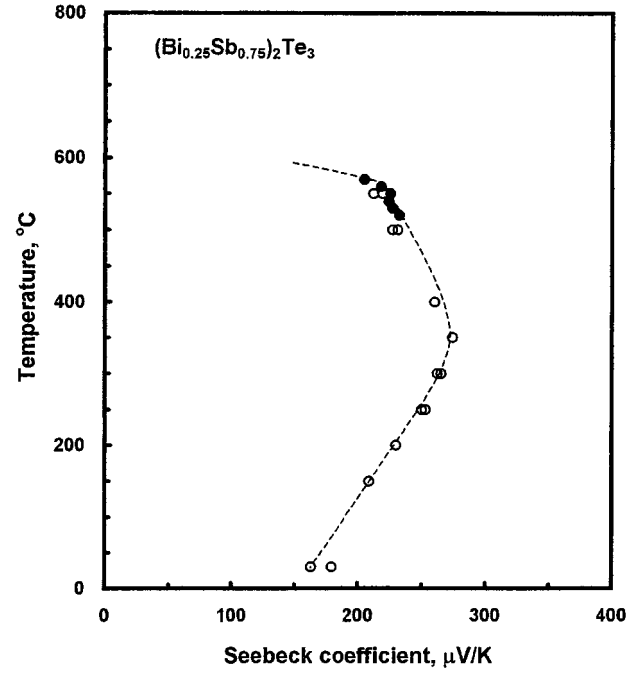

Figure 12 Equilibrium Seebeck coefficient of $(Bi_{0.25}Sb_{0.75})_2Te_3$ as a function of temperature.

Scherrer *et al*. [20] studied the equilibrium Seebeck coefficient of $(Bi_{0.25}Sb_{0.75})_2Te_3$ at the temperature range between 520°C and 570°C using the travelling heater method (THM), and reported that the hole concentration of $(Bi_{0.25}Sb_{0.75})_2Te_3$ decreases with decreasing annealing temperature. It means that the antistructure defect concentration, i.e. the solubility of Te in the matrix, depends on the temperature. Since the Seebeck coefficient of the heavily deformed specimens showed constant value of about 260 μV/K after annealing at 350°C as shown in Fig. 11, it could be thought as equilibrium Seebeck coefficient at that temperature. In Fig. 12, the Seebeck coefficient of the $(Bi_{0.25}Sb_{0.75})_2Te_3$ hot-pressed with mechanically alloyed powders, shown in Fig. 4, were compared with the data from Scherrer *et al*. [20]. Coincidence of the Seebeck coefficient of the hot-pressed specimens with those of the single crystals revealed that the equilibrium phases could be obtained by hot-pressing or annealing the mechanically alloyed powders.

The hole concentration of Sb_2Te_3-rich $(Bi,Sb)_2Te_3$ alloys is determined upon the antistructure defect concentration which is dependent upon the degree of Te-deficiency from the stoichiometric composition. Since the Seebeck coefficient of p-type thermoelectric materials is related with the hole concentration as Equation 1, the degree of Te-deficiency from the stoichiometric composition, i.e. a micro-phase diagram near the stoichiometric composition of $(Bi_{0.25}Sb_{0.75})_2Te_3$ can be evaluated. Fig. 13 illustrates the micro-phase diagram near the stoichiometric composition of $(Bi_{0.25}Sb_{0.75})_2Te_3$ solid solution.

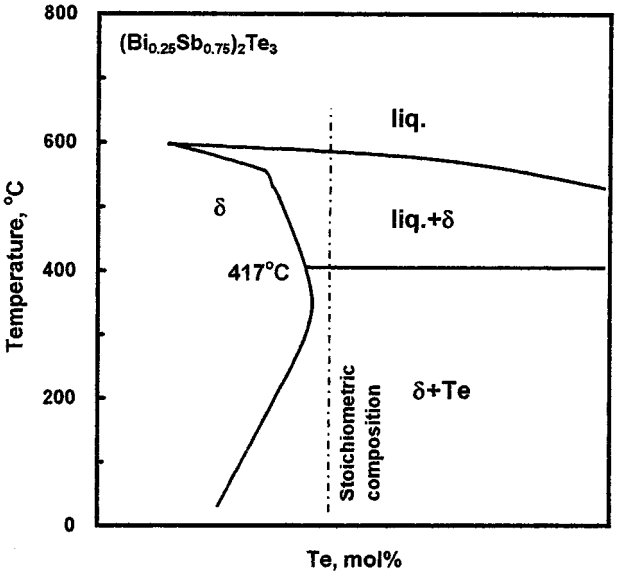

Figure 13 Micro-phase diagram near the stoichiometric $(Bi_{0.25}Sb_{0.75})_2Te_3$.

5. Conclusions

In the present work, the role of several factors which affect the Seebeck coefficient of the $(Bi_{0.25}Sb_{0.75})_2Te_3$ alloy during the hot-pressing has been elucidated. With the results of the Seebeck coefficient increase with hot-pressing of the cold-pressed compact, it could be thought that the formation of antistructure defects caused by evaporation of Te during hot-pressing would not be so significant to affect the carrier concentration. The Seebeck coefficient and the electrical resistivity of the hot-pressed specimen decreased after hydrogen reduction of the powders due to the increase in the hole concentration. Te vacancies formed by mechanical deformation significantly promote the diffusion of second phase Te atoms into their own lattice sites during hot-pressing process so that the matrix Te solubility approaches its equilibrium value at a given temperature in a relatively short length of time. Using the fact that the Seebeck coefficient of p-type $(Bi,Sb)_2Te_3$ alloys is related with the hole concentration, i.e. the concentration of antistructure defects, the micro-phase diagram near the stoichiometric composition of $(Bi_{0.25}Sb_{0.75})_2Te_3$ was evaluated. Te solubility is of conventional type and the solidus line is shifted from the stoichiometry toward bismuth and antimony in the (liq. $+\,\delta$) region.

References

1. H. J. GOLDSMID, in "CRC Handbook of Thermoelectrics," edited by D. M. ROWE (CRC Press, Boca Raton, 1995) p. 617.
2. W. M. YIM and F. D. ROSI, *J. Solid State Electronics* **15** (1972) 1121.
3. I. J. OHSUGI, T. KOJIMA and I. A. NISHIDA, *J. Appl. Phys.* **68** (1990) 5692.
4. K. HASEZAKI, M. NISHIMURA, M. UMATA, H. TSUKUDA and M. ARAAOKA, in Proceedings of the 12th International Conference on Thermoelectrics, Yokohama, Japan, November 1993, edited by K. Matsuura (1993) p. 307.
5. F. FUKUDA, A. ONODERA and H. HAGA, in Proceedings of the 12th International Conference on Thermoelectrics, Yokohama, Japan, November 1993, edited by K. Matsuura (1993) p. 24.
6. K. NAKAMURA, K. MORIKAWA, H. OWADA, K. MIURA, K. OGAWA and I. A. NISHIDA, in Proceedings of the 12th International Conference on Thermoelectrics, Yokohama, Japan, November 1993, edited by K. Matsuura (1993) p. 110.
7. A. YANAGITA, S. NISHIKAWA, Y. KAWAI, S. HAYASHIMOTO, N. ITOH and T. KATAOKA, in Proceedings of the 12th International Conference on Thermoelectrics, Yokohama, Japan, November 1993, edited by K. Matsuura (1993) p. 281.
8. B. Y. JUNG, S. E. NAM, D.-B. HYUN, J.-D. SHIM and T. S. OH, *J. Korean Inst. Met. & Mater*. **35** (1997) 153.
9. H. J. KIM, J. S. CHOI, D.-B. HYUN and T. S. OH, *ibid.* **35** (1997) 223.
10. T. C. HARMAN, J. H. CAHN and M. J. LOGAN, *J. Appl. Phys.* **30** (1959) 1351.
11. N. Kh. ABRIKOSOV, V. F. BANKINA, L. V. PORETSKAYA, L. E. SHELIMOVA and E. V. SKUDNOVA, in "Semiconducting II-VI, IV-VI, and V-VI Compounds" (Plenum Press, New York, 1969) p. 164.
12. J. S. BENJAMIN, *Sci. Amer*. **40** (1976) 234.
13. P. S. GILMAN and W. D. NIX, *Metall. Meyall. Trans. A* **12** (1981) 813.
14. M. ATZMAN, J. D. VERHOEREN, E. D. GIBSON and W. L. JOHNSON, *Appl. Phys. Lett*. **45** (1984) 1052.
15. H. J. GOLDSMID, in "Thermoelectric Refrigeration" (Plenum Press, New York, 1964) pp. 36–46.
16. W. D. KINGERY, H. K. BOWEN and D. R. UHLMANN, in "Introduction to Ceramics" (John Wiley & Sons, New York, 1976) p. 634.
17. G. R. MILLER and C.-Y. LI, *J. Phys. Chem. Solids* **26** (1965) 173.
18. M. I. TSIPIN and L. T. EVDOKIMENKO, *Izv. AN SSSR, Neorganicheskie Materiali* **19** (1973) 203.
19. J. M. SCHULTZ, J. P. McHUGH and W. A. TILLER, *J. Appl. Phys*. **33** (1962) 2443.
20. H. SCHERRER and S. SCHERRER, in Proceedings of the 12th International Conference on Thermoelectrics, Yokohama, Japan, November 1993, edited by K. Matsuura (1993) p. 90.

Received 9 January
and accepted 27 September 2000